ELSEVIER

Journal of Alloys and Compounds 323–324 (2001) 718–721

Journal of ALLOYS AND COMPOUNDS

www.elsevier.com/locate/jallcom

Vibronic oscillator strengths of Tm^{3+} in $Cs_2NaTmCl_6$

Peter A. Tanner[a,*], Roberto Acevedo[b], Oscar Hurtado[b], Teodoro Meruane[b]

[a]*Department of Biology and Chemistry, City University of Hong Kong, Tat Chee Avenue, Kowloon, Hong Kong SAR, PR China*
[b]*Facultad de Ciencias Físicas y Matemáticas, Universidad de Chile, Beaucheff 850, Casilla 2777, Santiago, Chile*

Abstract

Direct calculations (without variable fitting parameters) utilizing a symmetry-adapted vibronic crystal field–ligand polarization scheme are presented for the total vibronic oscillator strengths in the $^3H_6\ \Gamma_1 \rightarrow {}^3H_5$, $^3F_4$, $^1G_4$ absorption transitions of the Tm^{3+} ion in the cubic system $Cs_2NaTmCl_6$, and are in reasonable agreement with the experimental oscillator strengths from the 10 K absorption spectrum. The calculated total vibronic intensities are not particularly sensitive to the detailed compositions of electronic wavefunctions employed in the calculations, as long as the correct phases are employed. Experimental oscillator strengths for individual moiety mode transitions have been calculated, but in many cases these show large deviations from experimental values, particularly for ν_3 and ν_4 vibronic structure. Reasons for the failure of the model in this respect are considered.

Keywords: Insulators; Phosphors; Electron–phonon interactions; Optical properties; Light absorption and reflection

1. Introduction

The f–f transitions of lanthanide ions situated at centrosymmetric sites are rich in vibronic structure [1]. Several approaches have been utilized in calculating the vibronic intensities of these transitions [2–4]. The most direct method of calculation, developed by Acevedo and co-workers [5], is applied in the present study for the prediction of oscillator strengths, and of relative intensities, of several transitions in the absorption spectra of the cubic system $Cs_2NaTmCl_6$. Although measured and calculated vibronic oscillator strengths have been compared previously for the system $Cs_2NaYbCl_6$ [4], the present system has more numerous transitions between different multiplet terms, and thus provides a more comprehensive test of theory. Within the seven-system model, the form of the vibrational force field did not greatly affect the calculated vibronic intensity results for the $Cs_2NaYbCl_6$ system, so that a generalized valence force field (GVFF) has been employed throughout this work. The potential energy hypersurfaces associated with the terminal electronic states have roughly the same shape and are only vertically displaced from one another. Calculations have also been performed using the wavefunctions from different energy level parametrizations. Experimental oscillator strengths have been measured from the 10 K electronic absorption spectrum of polycrystalline samples of $Cs_2NaTmCl_6$ for comparison with the calculations.

2. Experimental

The preparation of polycrystalline $Cs_2NaTmCl_6$, and the measurement of the absorption spectra at 10 K, have been described previously [1]. Oscillator strengths, $\boldsymbol{P}_{if}$, of vibronic transitions were calculated from the spectral bands using the equation [3]

$$\boldsymbol{P}_{if} = 6.5033 \times 10^{-19} a^3 b^{-1} \int \boldsymbol{A}(\bar{\nu}) \mathrm{d}\bar{\nu} \quad (1)$$

where a is the lattice parameter (1061 pm at 10 K [6]), and b is the crystal thickness in cm. The refractive index, n, of $Cs_2NaTmCl_6$ was measured by immersion from 450 to 700 nm, and fitted to the equation

$$n = 1.584128 + 11819\lambda^{-2} \quad (2)$$

where λ is in nm.

3. Vibronic intensity calculations

The vibronic intensity calculations employed the combined crystal field (CF)–ligand polarization (LP) method, using a general valence force field for a seven-atom model,

*Corresponding author. Tel.: +852-2788-7840; fax: +852-2788-7406.
E-mail address: bhtan@cityu.edu.hk (P.A. Tanner).

0925-8388/01/$ – see front matter
PII: S0925-8388(01)01054-4

which has been described in detail elsewhere [3]. In view of our ignorance of the vibronic intensity sources, the closure approximation was employed, using a degenerate intermediate configuration energy of 93 000 cm^{-1}. Only a brief summary of the calculation is included here. The model considers only an isolated $TmCl_6^{3-}$ moiety at a site of octahedral symmetry, so that vibronic intensity contributions from lattice modes, or unit cell interactions, are not included. The performance of the model should be evaluated taking these considerations into account, as well as the fact that it does not include fitting parameters.

For absorption transitions from the $^3H_6$ Γ_1 electronic ground state (i) to the excited vibronic state $\Gamma_f + \nu_t$ (f), the calculated oscillator strength, $\boldsymbol{P}_{if}$, is given by

$$\boldsymbol{P}_{if} = 1.085 \times 10^{-11} \chi e^{-2} \Delta\bar{\nu}_f D_f(\nu_t) \quad (3)$$

where e is the electronic charge, χ is the effective field correction, which from (2) has values of 1.43, 1.44 and 1.49 for transitions to the terminal $^3F_4$, $^3H_5$ and $^1G_4$ levels, respectively;

$$\Delta\nu_f = \boldsymbol{E}(\boldsymbol{i} \rightarrow \boldsymbol{f}) + \bar{\nu}_t \quad (4)$$

where $\boldsymbol{E}(\boldsymbol{i} \rightarrow \boldsymbol{f})$ is the experimentally measured zero phonon line energy and $\bar{\nu}_t$ is the energy of vibration mode ν_t, taken as 269, 118 and 87 cm^{-1} for the odd-parity modes $t = 3$, 4 and 6, respectively. In Eq. (3), the dipole strength is

$$D_f(\nu_t) = |\langle \Phi_i | \boldsymbol{\mu}(\nu_t) | \Phi_f \rangle|^2 \quad (5)$$

where $\boldsymbol{\mu}(\nu_t)$ is factored into the electronic and vibrational parts. Furthermore, the electronic transition dipole moment, μ_T, contains two contributions from the crystal field and ligand polarization terms:

$$\mu_T = \mu_{CF} + \mu_{LP} \quad (6)$$

The dipole strength is thus comprised of three items, due to contributions from LP ($\boldsymbol{D}^{LP}$), CF ($\boldsymbol{D}^{CF}$) and cross-terms ($\boldsymbol{D}^{CT}$). In the case of the CF term, the master equation is

$$\mu_{i\rightarrow f}^{CF,\alpha}(\nu_t) = \sum_m \langle \Phi_i | U_{\nu_m}^{CF,\alpha} | \Phi_f \rangle L_{mt} \langle 0 | Q(\nu_t) | 1 \rangle \quad (7)$$

The electronic factors were calculated directly. The GF-matrix formalism was utilized to solve the vibrational problem, in order to determine the matrix elements L_{mt} relating normal coordinates to symmetry coordinates. Calculated oscillator strengths for individual vibronic origins then comprised products of squares of vibrational integrals involving the difference of one quantum of vibration, together with the square of the product of the electronic factor and the L-matrix element. In the case of the ν_t ($t = 3$, 4) modes of symmetry τ_{1u}, the mixing of the normal coordinates was thus taken into account.

4. Results and discussion

The $^3H_6 \rightarrow {}^1G_4$ absorption transition has previously been reported [10,11]. Fig. 1 shows new experimental data for the $^3H_6 \rightarrow {}^3F_4$, $^3H_5$ infrared absorption transitions in the 10 K absorption spectra of $Cs_2NaTmCl_6$, and the locations of zero phonon lines (ZPL) are indicated. The intensity of $^3H_6 \rightarrow {}^3F_4$ is mainly electric dipole vibronic in character, whereas that of $^3H_6 \rightarrow {}^3H_5$ is mainly magnetic dipole (intense ZPL not shown). The $^3H_6 \rightarrow {}^3F_4$ spectrum is at lower temperature, and more clearly resolved than previously reported. Each moiety-mode vibronic origin consists of several bands, assigned to the effects of longitudinal-optic mode splittings, dispersion and mode couplings. These vibrations are also marked in the figure for the different transitions. Table 1 summarizes the energies, with respect to the ZPL, and the relative intensities of the spectral bands assigned to each moiety mode. The latter are fairly constant for different transitions. The total

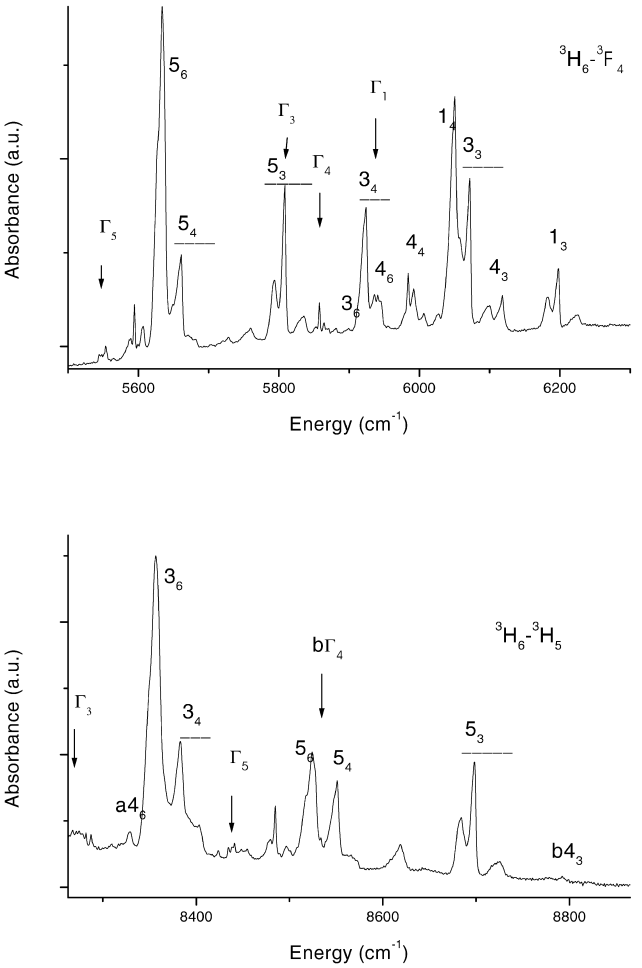

Fig. 1. Vibronic structure in the $^3H_6$ $\Gamma_1 \rightarrow \Gamma_f$($^3F_4$, $^3H_5$) absorption spectra of $Cs_2NaTmCl_6$. The positions of the electronic origins are marked with the irreducible representation of the excited state, and moeity mode vibronic structure is indicated by the terminal state notation: e.g. $a4_3$ represents $a\Gamma_4 + \nu_3$. The intense magnetic dipole origin $^3H_6$ $\Gamma_1 \rightarrow a\Gamma_4(^3H_5)$ at 8241 cm^{-1} has been omitted for clarity.

Table 1
Energies and approximate relative intensities of bands assigned to moiety mode vibronic origins

Mode	Energy (cm^{-1})	Description	Mean relative intensity (S.D.)
ν_3	245	Zone boundary/2-phonon	2.4 (0.4)
	260	TO	3.2 (1.0)
	285	LO	1.0
ν_4	111	TO	5.7 (1.5)
	130	LO/zone boundary/2-phonon	1.0
ν_6	78	Zone centre	1.0
	87	Zone boundary	4.8 (0.3)

vibronic oscillator strength measured for these transitions (i.e. excluding the intensity due to pure electronic transitions) is of the order 10^{-7} to 10^{-8} in each case (Table 2). The observed vibronic oscillator strengths summed over the individual ν_3, ν_4, and ν_6 moiety mode vibronic origins are also listed in Table 2 and are not greatly different from the total values. Total vibronic intensities calculated using three different sets of intermediate-coupling crystal field state wavefunctions (I, II and III) are included in Table 2. The wavefunctions labelled I correspond to those from the six-parameter energy level calculation of Tanner [10,11]. Set II are those resulting from a more sophisticated parametrization, with 10 variable parameters, which gave a smaller deviation in the energy level calculation in Ref. [1]. Set III are from a revised six-parameter model [12] which takes a consistent account of the relative phases of different wavefunctions in Ref. [13]. Set III are therefore very similar in composition to set II, except for several cases where the two wavefunctions are in antiphase. However, the relative phases differ, and are known to be incorrect in set I. For example, the $^3H_5$ Γ_3 crystal field state:

Wavefunction I: $-0.996|^3H_5\rangle - 0.049|^1G_4\rangle - 0.057|^3H_4\rangle$

Wavefunction II: $-0.997|^3H_5\rangle + 0.046|^1G_4\rangle - 0.054|^3H_4\rangle$

Wavefunction III: $+0.996|^3H_5\rangle - 0.053|^1G_4\rangle + 0.063|^3H_4\rangle$

wavefunctions II and III are in antiphase, but the phase of wavefunction I is different. The calculated total vibronic intensities (for ν_3, ν_4, and ν_6) are in remarkably good agreement with experiment for the transitions $^3H_6 \rightarrow {}^1G_4$, $^3F_4$, and in reasonable agreement with experiment for the transition with mainly magnetic dipole character, $^3H_6 \rightarrow {}^3H_5$. The detailed structure of the intermediate-coupled wavefunction (i.e. the comparison of sets II and III) is seen to make little difference. However, the different interference effects resulting from incorrect relative phases of wavefunctions does appear to lead to rather different calculated values (i.e. comparison of set I versus sets II and III). The following discussion is restricted to set II.

The calculated individual moiety mode vibronic oscillator strengths were generally in poor agreement with experiment for transitions to terminal $\Gamma_4 + \nu_t$ vibronic levels ($t = 3$, 4). The calculated oscillator strengths for ν_6 vibronic origins might be considered to be qualitatively acceptable, however (Table 3).

First, although the vibrational mixing of moiety modes

Table 2
Experimental and calculated vibronic oscillator strengths in the 10 K absorption spectrum of $Cs_2NaTmCl_6$[a]

Transition	Exptal. osc. str. ($\times 10^{-9}$)	Calc. osc. str. ($\times 10^{-9}$)			
	Total[b]	Moiety mode[c]	Calc. I	Calc. II	Calc. III
$^3H_6 \rightarrow {}^1G_4$	34.4	30.0	57.3	32.8	31.5
$^3H_6 \rightarrow {}^3F_4$	120	93	109.2	94.0	95.9
$^3H_6 \rightarrow {}^3H_5$	112	101	57.1	58.3	58.0

[a] Exptal. (Calc.) osc. str., experimental (calculated) oscillator strength; Calc. I–III, calculations I–III, refer to text.
[b] Total vibronic oscillator strength of the transition.
[c] Vibronic oscillator strength due to internal ν_3, ν_4 and ν_6 modes of $TmCl_6^{3-}$ moiety (Table 1).

Table 3
Experimental vibronic oscillator strengths for the $^3H_6\Gamma_1 \rightarrow {}^3F_4$, $^3H_5$, $^1G_4$ transitions of $Cs_2NaTmCl_6$[a]

Transition	Vibrational mode, ν_t	Oscillator strength ($\times 10^{-9}$) for transition to terminal state, $\Gamma_f + \nu_t$			
		Γ_1	Γ_3	Γ_4	Γ_5
$^3H_6$ $\Gamma_1 \rightarrow {}^3F_4$	ν_3	6.96	4.9	3.05	12.4
$^3H_6$ $\Gamma_1 \rightarrow {}^3F_4$	ν_4	19.1	9.71	$<9\times10^{-2}$	7.17
$^3H_6$ $\Gamma_1 \rightarrow {}^3F_4$	ν_6	ob (0)	<0.23 (1.6)	ob (1.3×10^{-3})	29.5 (14.0)
		Γ_3	bΓ_4	aΓ_4	Γ_5
$^3H_6$ $\Gamma_1 \rightarrow {}^3H_5$	ν_3	ob	0.89	ob	14.5
$^3H_6$ $\Gamma_1 \rightarrow {}^3H_5$	ν_4	16.9	<0.25	ob	10.4
$^3H_6$ $\Gamma_1 \rightarrow {}^3H_5$	ν_6	42.3 (5.9)	ob (2.2×10^{-2})	1.11 (9.1×10^{-3})	ob (1.5)
		Γ_1	Γ_3	Γ_4	Γ_5
$^3H_6$ $\Gamma_1 \rightarrow {}^1G_4$	ν_3	2.62	ob	0.576	1.65
$^3H_6$ $\Gamma_1 \rightarrow {}^1G_4$	ν_4	ob	2.68	0.286	1.88
$^3H_6$ $\Gamma_1 \rightarrow {}^1G_4$	ν_6	n.o. (0)	0.204 (0.38)	ob (1.3×10^{-3})	7.93 (5.5)

[a] n.o., not observed; ob, measurement is unreliable. Calculated values for ν_6 vibronic origins are in parentheses and utilized the electronic wavefunctions from the 10-parameter fit.

is taken into account in the calculation, the effects of dispersion are not. The experimental measurements clearly indicate that moiety-mode vibronic origins are not single bands, and the question of which spectral features (Table 1) actually constitute each vibronic origin is not generally agreed upon [7–9]. However, it would be expected that the measured intensity ratios of the same ν_t vibronic origin for different transitions might be in agreement with calculation, but this is not so. Thus the coupling of internal and external modes could differ for different transitions, or the intensity sources of the vibronic transitions are not accurately taken into account in the calculations. From our previous study of $Cs_2NaYbCl_6$, we consider that the effects of dispersion are not the major reason for the failure because the 'isolated ion' vibronic oscillator strengths (in $Cs_2NaGd_xYb_{1-x}Cl_6$, where x approaches 1) were not greatly different from those in the neat crystal.

The second reason for the failure of calculation may arise from the use of the closure approximation, since some particularly important intensity sources are neglected (when this approximation is adopted the nature of the intermediate central metal wavefunctions become irrelevant, except for the choice of an average effective energy). The complexity and ignorance of the $4f^{13}\,5d^9/4f^{11}\,6d$ configurations does not permit an evaluation to be made in this case. We have not attempted to improve the agreement with experiment by refining the effective baricentre energy.

A third reason for the failure of calculation could result from the mixing of vibronic states of the same overall symmetry representation, but of similar energy and usually involving different moeity modes. This would serve to redistribute intensity and enhance weaker transitions. However, the similarity of the lineshapes of a given vibronic origin in different electronic transitions may indicate that this novel source of improvement is not generally important. Furthermore, the more isolated transitions, where the mixing would be unimportant, do not provide agreement between theoretical and experimental oscillator strengths.

Even though the calculated intensities for the ν_6 vibronic origins are not in agreement with experiment, the agreement is considerably poorer for ν_4 and ν_3 vibronic origins. One mechanism which can provide and/or redistribute intensity for these two modes is the two-centre lanthanide–ligand correlated dipole interaction [14], following the initial f–d transition of the lanthanide ion. We will investigate the inclusion of these terms in a future study.

In conclusion, the simplicity of the first-order model calculation, using a seven-atom system, and without fitting parameters, provides a useful starting point for the assessment of vibronic intensity mechanisms, and gives reasonable results for the total vibronic intensities of term-to-term transitions. However, the method lacks accuracy in the prediction of individual vibronic origin intensities, and some reasons have been considered for the inaccuracies.

Acknowledgements

We acknowledge financial assistance from research grants: Hong Kong UGC Grant CityU 1067/99 to PAT; and Fondecyt Grant 1981207 and VRA of the Universidad Diego Portales Grants 2025 and 2049 to RA. We thank Chris S.K. Mak for technical assistance.

References

[1] P.A. Tanner, V.V.R.K. Kumar, C.K. Jayasankar, M.F. Reid, J. Alloys Comp. 215 (1994) 349.
[2] S.M. Crooks, M.F. Reid, P.A. Tanner, Y.Y. Zhao, J. Alloys Comp. 250 (1997) 297.
[3] R. Acevedo, P.A. Tanner, T. Meruane, V. Poblete, Phys. Rev. B 54 (1996) 3976.
[4] O.L. Malta, J. Phys. Chem. Solids 56 (1995) 1053.
[5] R. Acevedo, S.O. Vasquez, C.D. Flint, Mol. Phys. 74 (1991) 853.
[6] G.P. Knudsen, F.W. Voss, R. Nevald, H.-D. Amberger, in: G.J. McCarthy, H.B. Silber, J.J. Rhyne (Eds.), Rare Earths in Modern Science and Technology, Vol. 3, Plenum, New York, 1982.
[7] A. Barbanel, G.P. Chudnovskaya, I. Gavrish, R.B. Dushin, V.V. Kolin, V.P. Kotlin, J. Rad. Nucl. Chem. 143 (1990) 113.
[8] D.R. Foster, M.F. Reid, F.S. Richardson, J. Chem. Phys. 83 (1985) 3225.
[9] M. Bettinelli, C.D. Flint, Chem. Phys. Lett. 167 (1990) 45.
[10] P.A. Tanner, Mol. Phys. 53 (1984) 813, 835.
[11] P.A. Tanner, Mol. Phys. 54 (1985) 883.
[12] O. Hurtado, MSc Thesis, Department of Basic Chemistry, University of Chile, 1998.
[13] J.S. Griffith (Ed.), The Theory of Transition Metal Ions, Cambridge University Press, 1980, p. 393.
[14] J. Dexpert-Ghys, F. Auzel, J. Chem. Phys. 80 (1984) 4003.